Hybrid Signal-based and Geometry-based Prediction for Haptic Data Reduction

Xiao Xu, Julius Kammerl, Rahul Chaudhari and Eckehard Steinbach
Institute for Media Technology,
Technische Universität München,
Germany
Email: {xiao.xu, kammerl, rahul.chaudhari, eckehard.steinbach}@tum.de

***Abstract*—Haptic data reduction schemes address the high packet-rate requirements of networked haptics. Perception-driven predictive coding approaches enable strong packet rate reduction while keeping the introduced distortion below human haptic perception thresholds. The performance of predictive coding is strongly influenced by factors such as human behavior, system characteristics, geometric and impedance properties of the environment, etc. In this paper, we first describe a novel surface geometry-based prediction approach for haptic data reduction where local object surface features are approximated with the help of simple geometric models. Secondly, we present a hybrid framework that combines signal-based and geometry-based prediction. Psychophysical experiments are performed to validate this framework. The results of the proposed geometry-based prediction show an improvement in haptic data reduction of about 54% as compared to the signal-based prediction (linear predictor). Furthermore, the presented hybrid prediction technique allows for an additional gain of 15%.**

I. Introduction

A telepresence and teleaction (TPTA) system is composed of two main parts: a human operator (OP) / master system and a teleoperator (TOP) / slave system [1]. The TOP is controlled by the OP while interacting with the remote environment. The two subsystems exchange haptic data over the network, as visualized in Fig. 1. The user movement (position / velocity) captured by a haptic device at the OP side commands a slave robot at the TOP side. The slave follows these commands and returns the force (and torque) feedback signals sensed during its interaction with the remote environment. The haptic device displays the force and torque to the OP through the haptic device which allows him to haptically immerse into the remote environment.

For real-time haptic teleoperation, haptic signals on either side of the communication channel need to be sampled (and packetized immediately) with a rate of 1 kHz. This is necessary for stability as well as transparency reasons [2]. When running a TPTA system across a packet-based communication network, such a high packet rate as well as the additional data overhead due to the transmission of packet header information lead to inefficient communication.

Early approaches addressing haptic data compression can be found in [3]. These approaches, however, concentrate on the statistical properties of haptic signals. The first perceptual deadband-based approach for real-time haptic data compression has been presented in [4], [5], [6] and investigated in terms of stability criteria in [7] and [8]. In [9], a linear predictor has been added to further reduce the haptic velocity and force-feedback packet rates. Signal-based prediction methods in combination with the deadband approach to further reduce the haptic data rate are presented in [10] and [11]. In [12], a model-mediated approach is presented to render the haptic signal locally with a geometric model of remote objects for a TPTA system with significant communication delay. In [13], a geometry model-based predictive coding extension for the deadband approach has been briefly mentioned, which predicts the signal samples based on the surface geometric structure and impedance of the remote objects. This allows for local rendering of the remotely generated or sensed haptic force-feedback values.

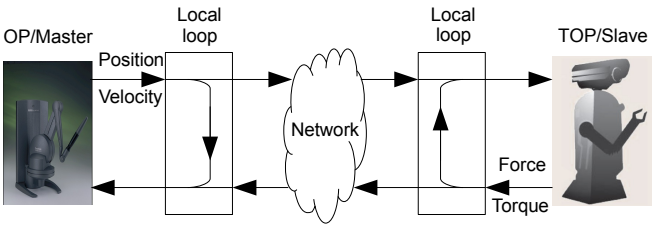

Fig. 1. Structure overview of the TPTA system (adapted from [1]). Image source: http://www.sensable.com/haptic-phantom-desktop.htm

In this paper, we make two contributions. Firstly, we provided a detailed description of the surface geometry-based prediction approach for haptic data reduction which was briefly described earlier in [13]. In this approach, local object surface features are estimated by simple geometric primitives. This allows for local rendering of the haptic signals and further reduces the packet rate of the haptic data in comparison to signal-based prediction. Secondly, we combine signal-based and geometry-based prediction in a hybrid framework that switches between the predictors adaptively. The hybrid prediction method enhances the subjective quality along with a further reduction of packet rate with respect to each individual predictor.

The rest of this paper is organized as follows: Section 2 reviews briefly the perceptual deadband haptic data reduction approach. Section 3 details various predictive coding algorithms including signal-based and geometry-based predictors.

The structure of the proposed hybrid prediction framework is explained in Section 4. Section 5 describes the psychophysical tests conducted to validate the hybrid prediction framework. The experimental results are discussed and analyzed in Section 6. We conclude this paper in Section 7 with a summary of the results and ideas for future work.

II. Perceptual Haptic Data Reduction

A. Weber's Law

Weber's law describes the perceivability of the change of a stimuli in a pairwise comparison of the stimuli ([14], [15]). The size of the difference threshold, or just noticeable difference (JND), is expressed as a linear function of stimulus intensity. This relationship can be represented by the following equation:

$$\frac{\Delta I}{I} = k = constant$$

where I is the stimulus intensity, ΔI is the change in stimulus intensity which is perceivable just as often as it is not and k is a constant called the Weber factor. With some variation, Weber's law has been found to apply to most of the human senses including the haptic sense [15].

B. Perceptual Deadband Coding

Weber's law has been exploited for haptic data reduction by the lossy deadband coding approach in [6]. The deadband encoder outputs a haptic sample for transmission only when it exceeds the JND with respect to the last transmitted sample value. Otherwise, nothing is transmitted. On the decoder side, the incoming haptic signal is reconstructed in the following manner. When a sample value is received, it is sent for display to the haptic device. At other sampling instants when no update is received, the last received haptic sample is held. The principle of the deadband approach is illustrated in Fig. 2. The black filled circles represent sample values that require transmission according to the deadband coding algorithm. The haptic samples represented by empty circles, on the other hand, do not require transmission, as they do not constitute perceivable changes in the haptic signal.

III. Predictive Coding

In order to further reduce the number of transmitted packets, a prediction scheme for haptic signals can be employed. Only if the predicted haptic sample values differ from the incoming signal value by more than the JND, the prediction error needs to be communicated [9], [6]. In this paper, we discuss two different prediction methods, a signal-based and a novel geometry-based prediction method.

A. Signal-based Prediction

For the signal-based prediction, we deploy two prediction modes: the zero-order-hold (ZOH) mode and the linear first order mode. The zero order prediction is described in Section II-B. The linear predictor [9] works as follows,

$$f_i = \begin{cases} f_{new} & \text{new value arrived} \\ f_{i-1} + \frac{f_{new-1} - f_{new-2}}{t_{new-1} - t_{new-2}}(t_i - t_{i-1}) & \text{else} \end{cases}$$

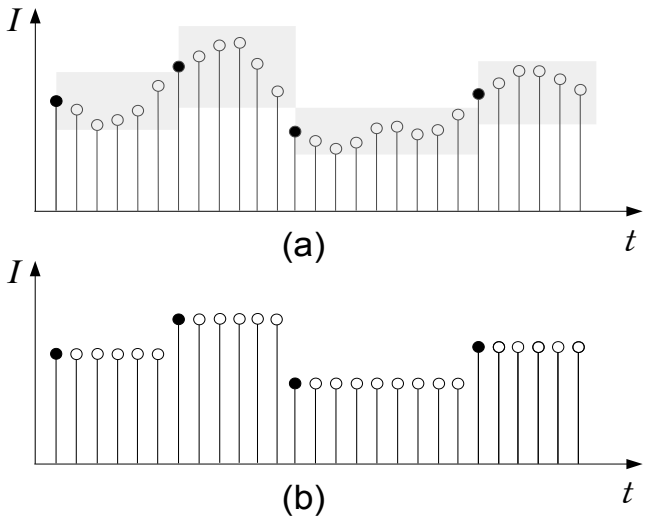

Fig. 2. 1-DoF deadband approach as described in [6]. The input signal (a) is downsampled and only the values represented with black filled circles are transmitted. In (b), the output signal is upsampled using the zero-order-hold method.

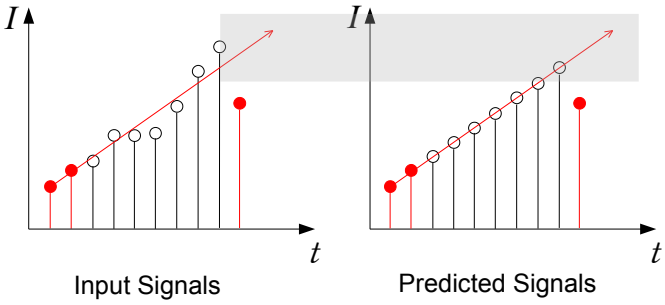

Fig. 3. Principle of linear prediction. The red values are transmitted and used to predict the current haptic value. If the predicted value differs by more than the JND from the actual value, a new value is transmitted and the predictor is updated.

where $\{f_i, f_{i-1}, f_{i-2}, \dots\}$ are the most recent prediction force values given by the predictor and $\{t_i, t_{i-1}, t_{i-2}, \dots\}$ are the corresponding time instances. $\{f_{new}, f_{new-1}, f_{new-2}, \dots\}$ and $\{t_{new}, t_{new-1}, t_{new-2}, \dots\}$ are the last received forces and the corresponding time instances, respectively. According to the formula above, the predicted force value lies on a straight line determined by the last two received force values (Fig. 3). Once the difference between the predicted value and the actual value is larger than the JND, a new value f_{new} is transmitted and the parameters of the predictor are updated accordingly.

B. Geometry-based Prediction

While touching a surface, we perceive important information such as position, stiffness, friction, etc. We may use this information to also predict contact points on the same surface that we have not touched yet. Inspired by this observation, we propose a geometry-based prediction method which predicts future signal samples based on a locally valid geometry model which is built from previous contact points with the

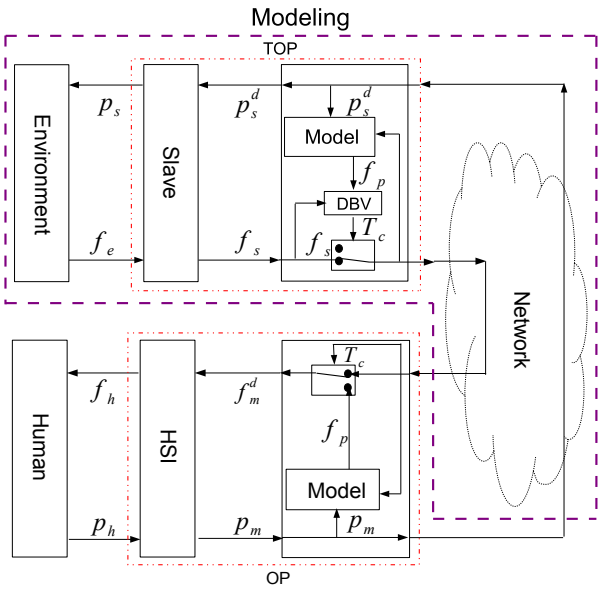

Fig. 4. Principle of geometry-based prediction. Force-position pairs are used to estimate prediction models describing geometric and impedance properties of the environment. The model is used to describe the combined impedance of the network and the slave in contact with the environment.

remote object. This model is solely based on transmitted haptic signals, without the need for transmitting additional side information. By combining absolute position and remotely received force-feedback information, we are able to model geometric and physical properties of the teleoperator contact with the remote environment. Similar to the concept of model-mediated telemanipulation [12], this allows for predicting the haptic signals by locally rendering the contact events. In this context, the parameter values of such local models should be estimated as quickly as possible in order to ensure control-loop stability and transparency. These requirements demand simple models with small parameter sets.

Our proposed scheme is illustrated in Fig. 4. On the master side, $\boldsymbol{p_h}$ denotes the position command by the human and $\boldsymbol{p_m}$ the resulting master position. On the slave side, $\boldsymbol{p_s^d} = \boldsymbol{p_m}$ denotes the desired slave position, while $\boldsymbol{p_s}$ denotes the actual resulting slave position. On the other hand, $\boldsymbol{f_e}$ denotes the contact force with the remote environment, while $\boldsymbol{f_s}$ denotes the force sensor output. $\boldsymbol{f_m^d} = \boldsymbol{f_s}$ denotes the desired force feedback, with $\boldsymbol{f_h}$ denoting the actual force applied to the human operator.

The deployed model predicts the force feedback signal $\boldsymbol{f_p}$ based on the incoming position signal $\boldsymbol{p_s^d}$ (=$\boldsymbol{p_m}$) at both, the master and the slave side. At the slave side, the model prediction is used to evaluate the correctness of the prediction. Only if the difference between the predicted force $\boldsymbol{f_p}$ and the actual force $\boldsymbol{f_s}$ exceeds the applied perception thresholds (decided by the deadband verification - DBV), we transmit haptic signals (controlled by the trigger signal T_c). Accordingly, the master can display the predicted samples as long as no haptic updates are received.

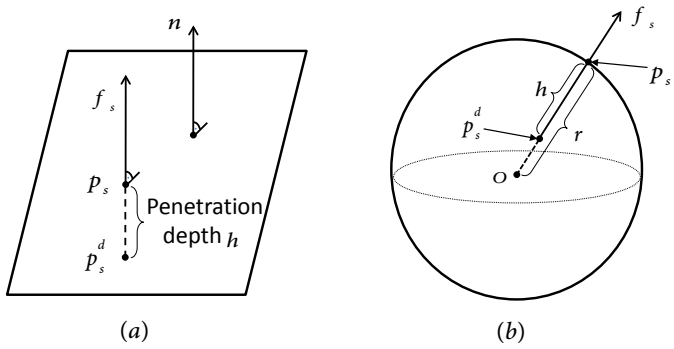

Fig. 5. Device position and its penetration depth for the plane model (a) and sphere model (b).

Model estimation & haptic rendering

In order to locally predict remote force feedback based on the sensed position signal $\boldsymbol{p_s^d}$, we need to model the geometric and impedance properties of the environment. Note that the modeled impedance properties represent the combined impedance of the network and the slave in contact with the environment (see Fig. 4). In the following, we show that by combining the desired slave position $\boldsymbol{p_s^d}$ and the corresponding measured force feedback signal $\boldsymbol{f_s}$, we are able to estimate the parameters of our prediction models.

To minimize the amount of samples necessary for estimating remote objects, our models only focus on the displayed stiffness and geometric surface structure of non-deformable objects. We neglect surface friction, slave inertia and network delay. Furthermore, the geometric characteristics of the environment are modeled with the help of simple planar and spherical models for describing planar, convex and concave surface structures. In the following, we describe these models in more detail.

Plane model

A plane surface in 3D space can be expressed as follows:

$$ax + by + cz + d = 0 \tag{1}$$

where $\boldsymbol{n} = (a, b, c)$ is the normal vector of the plane (see Fig. 5 (a)). In absence of surface friction, the direction of the actual force $\boldsymbol{f_s} = (f_x, f_y, f_z)$ is identical to the plane normal $\boldsymbol{n}$. So $\boldsymbol{n} = (\frac{f_x}{|\boldsymbol{f_s}|}, \frac{f_y}{|\boldsymbol{f_s}|}, \frac{f_z}{|\boldsymbol{f_s}|})$.

Furthermore, assuming that we know the stiffness of the slave in contact with the environment, we can use Hooke's law to estimate the surface contact point $\boldsymbol{p_s}$

$$\boldsymbol{p_s} = \boldsymbol{f_s}/s + \boldsymbol{p_s^d}$$

Where $\boldsymbol{p_s^d} = (p_x, p_y, p_z)$ and s is the stiffness. Combined with (1), we get

$$(\frac{f_x^2}{|\boldsymbol{f_s}|} + \frac{f_y^2}{|\boldsymbol{f_s}|} + \frac{f_z^2}{|\boldsymbol{f_s}|}, 1)\begin{pmatrix} 1/s \\ d \end{pmatrix} = (\frac{f_x p_x}{|\boldsymbol{f_s}|} + \frac{f_y p_y}{|\boldsymbol{f_s}|} + \frac{f_z p_z}{|\boldsymbol{f_s}|})$$

In this equation the only unknown variables are the stiffness s and plane parameter d. Therefore, by collecting at least two

force-position pairs, and solving a system of linear equations, we can define the plane model (Fig. 6 (left)).

In order to use the model for local haptic rendering, the penetration depth h can be computed as follows:

$$h = \frac{|ap_x + bp_y + cp_z + d|}{\sqrt{a^2 + b^2 + c^2}}$$

If $h > 0$, the current device point is outside the object. So the predicted force should be 0, otherwise the predicted force can be computed by Hooke's law:

$$\begin{cases} h \geq 0 \;\Rightarrow\; |\boldsymbol{f_p}| = 0 & \text{not touched} \\ h < 0 \;\Rightarrow\; |\boldsymbol{f_p}| = s \cdot h & \text{touched} \end{cases}$$

Sphere model

A sphere is defined by the center $\boldsymbol{o} = (o_x, o_y, o_z)$ and its radius r (Fig. 5 (b)).

The point $\boldsymbol{p_s} = \boldsymbol{o} + \boldsymbol{r}$ should lie on the sphere's surface. Under the assumption of no surface friction, the actual force $\boldsymbol{f_s}$ points from the center $\boldsymbol{o}$ of the sphere, radially outward. Taking Hooke's law into account, we can get the force sample into the equation:

$$\boldsymbol{o} + \boldsymbol{r} - \boldsymbol{f_s}/s = \boldsymbol{p_s^d}$$

where $\boldsymbol{r} = r\frac{\boldsymbol{f_s}}{|\boldsymbol{f_s}|}$. In matrix-vector notation form,

$$\begin{pmatrix} 1 & 0 & 0 & \frac{f_x}{|\boldsymbol{f_s}|} & -f_x \\ 0 & 1 & 0 & \frac{f_y}{|\boldsymbol{f_s}|} & -f_x \\ 0 & 0 & 1 & \frac{f_z}{|\boldsymbol{f_s}|} & -f_x \end{pmatrix} \begin{pmatrix} o_x \\ o_y \\ o_z \\ r \\ 1/s \end{pmatrix} = \begin{pmatrix} p_x \\ p_y \\ p_z \end{pmatrix}$$

Here we have five unknown variables and three equations. Therefore, to solve this system of linear equations, we again need at least two force-position pairs.

In order to use the sphere model for force prediction, we need to determine the penetration depth h and the force direction. If $s > 0$, the surface is convex, otherwise it is concave. So depending upon whether we are in contact with a virtual object or not, and whether we have determined a convex or a concave surface model, the predicted force $\boldsymbol{f_p}$ can be computed as:

$$\boldsymbol{f_p} = \begin{cases} ||\boldsymbol{p_s^d} - \boldsymbol{o}| - r| \cdot s \cdot \frac{\boldsymbol{p_s^d} - \boldsymbol{o}}{|\boldsymbol{p_s^d} - \boldsymbol{o}|} & \text{if } |\boldsymbol{p_s^d} - \boldsymbol{o}| < r,\ s > 0 \\ ||\boldsymbol{p_s^d} - \boldsymbol{o}| - r| \cdot s \cdot \frac{\boldsymbol{o} - \boldsymbol{p_s^d}}{|\boldsymbol{o} - \boldsymbol{p_s^d}|} & \text{if } |\boldsymbol{p_s^d} - \boldsymbol{o}| > r,\ s < 0 \\ 0 & \text{else} \end{cases}$$

Fig. 6 (right), shows an example of a local sphere model of the object surface.

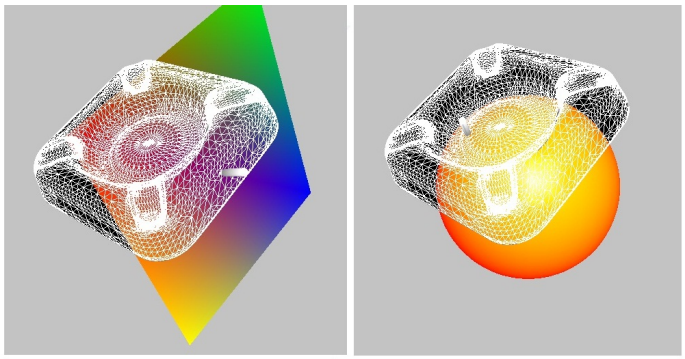

Fig. 6. Geometric plane (left) and sphere (right) models are built from the received force-position pairs. With these models the predictor at both the TOP and the OP sides can render the haptic force locally, if the JND threshold is not violated.

IV. Hybrid predictor

So far we have introduced four kinds of predictors (ZOH, linear, plane-based and sphere-based). These predictors show different performance in different situations. For example, if the remote object exhibits simple geometric surfaces, e.g. a wall, a desk or a rigid ball or edge, etc, the geometric predictors outperform the signal-based prediction. On the other side, if the surface consists of complex structures, the signal-based prediction performs better. In addition, the user's exploration strategy (tapping, moving along the surface, pressing, etc.) can also strongly affect the performance of the predictors. In order to select the best prediction scheme which would allow best possible data reduction performance, we propose a hybrid prediction framework. In our hybrid prediction scheme, network transmission is only triggered if a new haptic signal update needs to be transmitted.

The hybrid prediction runs all 4 predictors in parallel. It is based on a decision function combined with a hold-last-selected-predictor strategy. The decision function is expressed as,

$$w_i = |(\boldsymbol{f_p^i} - \boldsymbol{f_s})|/|\boldsymbol{f_s}|$$

where w_i is the error value for the ith predictor, $\boldsymbol{f_p^i}$ is the predicted force from the ith predictor and $\boldsymbol{f_s}$ is the actual force from the TOP. This enables us to select the jth predictor, which has the smallest prediction error w_j.

With the hold-last-selected-predictor strategy, the current prediction scheme is used until the predicted signal violates the applied perception bounds. With the transmitted packet, all the predictors are updated and the new prediction scheme is selected according to the decision function.

V. Subjective tests

In order to evaluate the performance of the proposed prediction methods, we developed a virtual environment for simulating the TPTA system. In psychophysical experiments with this virtual environment, we investigate the subjective quality and performance of the presented perceptual haptic data reduction techniques.

TABLE I
RATING SCHEME

Description	Rating
no difference	5
perceptible, but not disturbing	4
slightly disturbing	3
disturbing	2
strongly disturbing	1
completely distorted	0

A. Subjects

A total of fourteen subjects participated in the psychophysical tests, ranging in age from 23-32. All of them were right-handed. Ten of them were males, while the rest were females. Ten of them had never used a haptic device before and the remaining four had used such a device on a regular basis.

B. Experimental procedure

In order to standardize tests across subjects, during the experiment, specific instructions regarding the seating posture and the hand-device configuration were given. The computer screen displaying the VE was placed in front of the participant while the haptic device was placed on the right. A cardboard screened the haptic device from visual observation by the subjects. The participants also wore headphones playing music to mask the noise emanating from the motor of the haptic device. This was done in order to ensure that the subjects responded only to haptic stimuli, while giving psychophysical ratings.

The test software uses the CHAI3D library (www.chai3d.org). The simulated environment contains a 3D model (see Fig. 6) which can be haptically explored. The SensAble PHANTOM DESKTOP^{TM} haptic device is used for the experiments. In the experiments, we used Weber factors of 2.5%, 5%, 10%, 15%, 20%, 30% for configuring the perceptual haptic data reduction. During the experiment, subjects should give a rating from level 0 to 5 (Table 1) according to the quality of the displayed haptic sensations.

At the beginning of the experiment, a training session was conducted with the subjects to familiarize them with the experimental settings and the task to be performed. The subjects were guided to recognize the distortion artifacts introduced by the deadband coding scheme and its combination with various prediction modes. Here the best possible haptic feedback (0% Weber factor, designated level 5), an intermediate quality haptic feedback(12.5% Weber factor, ZOH prediction, designated level 3) and a bad quality haptic feedback (25% Weber factor, linear prediction, designated level 1) were displayed to the subjects as references. In the experimental phase, each subject was required to perform 30 tests (six different Weber factors for each one of the five prediction methods: ZOH, linear, plane, sphere and hybrid). The parameters of the predictors and the Weber factors were chosen randomly. In each test, the subject was allowed a time frame of 10 seconds to tap or move across a certain region of the virtual object. After each test, the participant gave a feedback rating for this test. The whole experiment lasted around 30 minutes (including introduction and training). After every 10 tests there was a break for the subjects.

VI. RESULTS

The packets rate vs. Weber factors for various prediction modes are shown in Fig. 7. The subjective rating results for the various predictors across the considered range of Weber factors are shown in Fig. 8. The hybrid and geometry-based predictors perform better and show a higher compression ratio in comparison to the signal-based prediction for the same Weber factor. Especially, compared to the ZOH predictor, at a Weber factor of 10% we observe a data reduction of about 31% for the plane-based prediction, 18% for the sphere-based prediction and 42% for the hybrid predictor while the subjective quality are all about 30% higher.

In Fig. 8, there is no significant subjective quality difference between the hybrid prediction and the geometry-based prediction. But these prediction methods have higher qualities than the signal-based prediction, especially for large Weber factors (see Weber factors 20% and 30%). In our observation, the subjective quality is adversely affected by disturbances caused by sudden force-changes due to the updating of predictors. During the experiment we observed that under large Weber factors the hybrid and geometry-based prediction generate reduced disturbances; their update rates are much lower than those for the signal-based prediction.

In Fig. 9, the subjective quality vs. packet rate curves (Q-R curve) are shown, where the hybrid prediction consistently outperforms the other prediction methods. In terms of subjective quality, the hybrid prediction performs best and always gives a better subjective feeling at comparable packet rates. The hybrid prediction also achieves a higher compression ratio in comparison to the other individual predictors. At the subjective quality level 4 (good quality), by using geometry-based prediction the haptic data reduction is about 54% and 60% as compared to the linear and ZOH predictors, respectively. Furthermore, the hybrid prediction shows an additional gain of about 15% in comparison to the geometry-based prediction method.

VII. CONCLUSION AND FUTURE WORK

This paper details our geometry-based prediction for deadband-based haptic data reduction and combines it with a previously proposed signal-based predictor in a hybrid framework. The geometry-based prediction allows for local rendering of remote haptic signals. The hybrid prediction scheme dynamically selects the best predictor in terms of subjective quality and packet rate reduction. Conducted experiments show significant improvements in performance when using the geometry-based prediction models. Additional gains can be achieved with the hybrid prediction framework.

In future work, we will include additional model parameters such as friction and dynamic environments. In addition, we

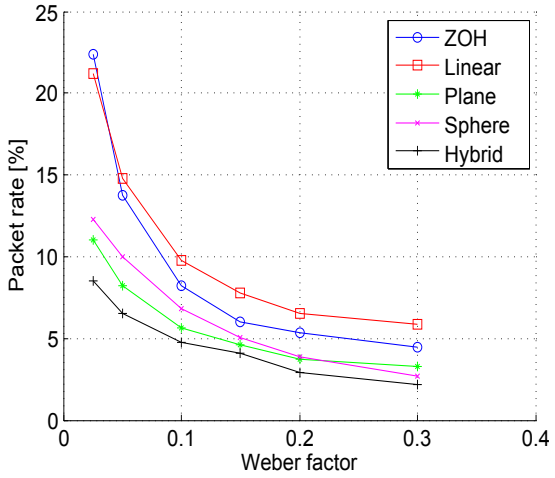

Fig. 7. The packet rate curve for all 5 prediction modes. The hybrid prediction mode leads to the lowest packet rate.

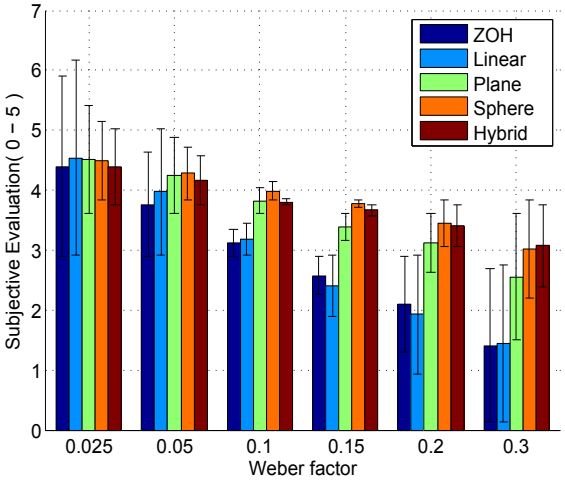

Fig. 8. Mean subjective ratings and standard deviation for all prediction modes. There is no significant difference between the hybrid prediction and the best one (sphere-based prediction).

will investigate real-world TPTA scenarios with communication delay.

ACKNOWLEDGMENT

This work has been supported, in part, by the European Research Council under the European Unions Seventh Framework Programme (FP7/2007-2013) / ERC Grant agreement no. 258941, and in part, by the German Research Foundation (DFG) under the project STE 1093/4-1.

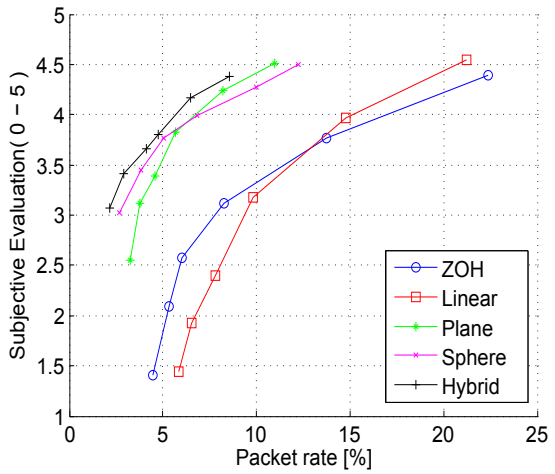

Fig. 9. The Q-R curve. The hybrid prediction performs always better than the other 4 prediction modes.

REFERENCES

[1] W. R. Ferrell and T. B. Sheridan, "Supervisory control of remote manipulation," *IEEE Spectrum*, vol. 4, no. 10, pp. 81–88, October 1967.

[2] J. E. Colgate, P. E. Grafing, M. C. Stanley, and G. Schenkel, "Implementation of stiff virtual walls in force-reflecting interfaces," in *Proc. of the Virtual Reality Annual International Symposium*, pp. 202–208, Seattle, WA, September 1993.

[3] C. Shahabi, A. Ortega, and M. R. Kolahdouzan, "A comparison of different haptic compression techniques," in *Proc. of the IEEE International Conference on Multimedia & Expo (ICME)*, vol. 1, pp. 657–660, Lausanne, Switzerland, August 2002.

[4] P. Hinterseer, E. Steinbach, S. Hirche, and M. Buss, "A novel, psychophysically motivated transmission approach for haptic data streams in telepresence and teleaction systems," in *Proc. of the IEEE International Conference on Acoustics, Speech and Signal Processing (ICASSP)*, vol. 2, pp. 1097–1100, Philadelphia, PA, USA, March 2005.

[5] P. Hinterseer and E. Steinbach, "A psychophysically motivated compression approach for 3D haptic data," in *Proc. of the International Symposium on Haptic Interfaces for Virtual Environment and Teleoperator Systems (HAPTICS)*, pp. 35–41, Arlington, VA, USA, March 2006.

[6] P. Hinterseer, S. Hirche, S. Chaudhuri, E. Steinbach, and M. Buss, "Perception-based data reduction and transmission of haptic data in telepresence and teleaction systems," *IEEE Trans. on Signal Processing*, vol. 56, no. 2, pp. 588–597, February 2008.

[7] S. Hirche, P. Hinterseer, E. Steinbach, and M. Buss, "Transparent data reduction in networked telepresence and teleaction systems. part 1: Communication without time delay," *Presence: Teleoperators & Virtual Environments*, vol. 16, no. 5, pp. 523–531, October 2007.

[8] M. Kuschel, P. Kremer, S. Hirche, and M. Buss, "Lossy data reduction methods for haptic telepresence systems," in *Proc. of the International Conference on Robotics and Automation (ICRA)*, pp. 2933–2938, May 2006.

[9] P. Hinterseer, E. Steinbach, "Model-based data compression for 3D virtual haptic teleinteraction," in *Proc. of the International Conference on Consumer Electronics (ICCE)*, pp. 23–24, Las Vegas, NV, USA, January 2006.

[10] S. M. Clarke, G. Schillhuber, M. F. Zaeh, and H. Ulbrich, "Prediction-based methods for teleoperation across delayed networks," *Multimedia Systems*, vol. 13, no. 4, pp. 253–261, 2008.

[11] N. Sakr, J. Zhou, N. Georganas, J. Zhao, and X. Shen, "Prediction-based haptic data reduction and compression in tele-mentoring systems in telementoring systems," *IEEE Trans. on Instrumentation and Measurement*, vol. 58, no. 5, pp. 1727–1736, May 2008.

[12] P. Mitra and G. Niemeyer, "Model mediated telemanipulation," *International Journal of Robotics Research*, vol. 27, no. 2, pp. 253–262, February 2008.

[13] E. Steinbach, S. Hirche, J. Kammerl, I. Vittorias, and R. Chaudhari, "Haptic data compression and communication," *IEEE Signal Processing Magazine, IEEE*, vol. 28, no. 1, pp. 87–96, January 2011.

[14] E. Weber, *Die Lehre vom Tastsinn und Gemeingefuehl, auf Versuche gegruendet*, Braunschweig, Germany: Vieweg, 1851.

[15] G. A. Gescheider, *Psychophysics*, Lawrence Erlbaun, 1985.